Bulletin of the Seismological Society of America, Vol. 85, No. 5, pp. 1507–1512, October 1995

Numerical Source Implementation in a 2D Finite Difference Scheme for Wave Propagation

by O. Coutant, J. Virieux, and A. Zollo

Abstract We describe how to implement seismic sources in a 2D staggered grid of a finite difference scheme of *P-SV* wave propagation. By comparison with analytical solutions in a homogeneous medium, we show that a very simple numerical description of sources in a second-order scheme provides good accuracy for radiated waves if one takes the elementary length where 2D stresses are applied as the grid step of the numerical scheme. The accuracy will depend on the grid step and the time step. The error is less than 10% and depends on the azimuth to the station.

Introduction

Finite difference modeling of wave propagation has been improved in the last 10 years. Second-order accurate finite difference of derivative operators (Kelly *et al.*, 1976; Virieux, 1984; Virieux, 1986) has been replaced by schemes of higher order (Bayliss *et al.*, 1986; Dablain, 1986; Levander, 1988; Crase, 1990), by schemes with precision in a limited frequency band (Holberg, 1987), or by pseudospectral schemes (Kosloff and Baysal, 1982; Kosloff *et al.*, 1984; Kosloff *et al.*, 1989). While these works describe the numerical scheme for wave propagation, the numerical excitation of the grid by a seismic source has never been completely presented, and published examples often reduce to the computation of seismograms for an explosive source. Since the work of Vidale and Helmberger (1987) for more complex types of seismic sources based on a numerical implementation of Alterman and Karal (1968) and used by Alford *et al.* (1974), very little attention has been focused on numerical source description. We shall present in this note a numerical implementation of seismic sources with special attention to earthquake double-couple sources much simpler than the numerical scheme of Vidale and Helmberger (1987). By comparison with complete analytical solutions in a homogeneous medium, we shall check the accuracy of this implementation.

Force and Dislocation Source Implementation

Since the work of Alterman and Karal (1968), in which the incident analytical wave is subtracted from the numerical solution in the homogeneous source region in order to avoid artificial reflections, many researchers have implemented seismic sources differently. For example, Kosloff *et al.* (1989) added external forces through the time evolution of the velocity as usual in elastodynamic equations given by the following:

$$\rho \frac{\partial \upsilon_x}{\partial t} = \frac{\partial \tau_{xx}}{\partial x} + \frac{\partial \tau_{xz}}{\partial z} + \mathbf{f}_x, \tag{1}$$

$$\rho \frac{\partial \upsilon_z}{\partial t} = \frac{\partial \tau_{xz}}{\partial x} + \frac{\partial \tau_{zz}}{\partial z} + \mathbf{f}_z, \tag{2}$$

$$\frac{\partial \tau_{xx}}{\partial t} = (\lambda + 2\mu) \frac{\partial \upsilon_x}{\partial x} + \lambda \frac{\partial \upsilon_z}{\partial z}, \tag{3}$$

$$\frac{\partial \tau_{zz}}{\partial t} = (\lambda + 2\mu) \frac{\partial \upsilon_z}{\partial z} + \lambda \frac{\partial \upsilon_x}{\partial x}, \tag{4}$$

$$\frac{\partial \tau_{xz}}{\partial t} = \mu \left(\frac{\partial \upsilon_x}{\partial z} + \frac{\partial \upsilon_z}{\partial x} \right), \tag{5}$$

where (υ_x, υ_z) is the 2D velocity vector and $(\tau_{xx}, \tau_{zz}, \tau_{xz})$ are the components of the stress tensor. The medium is characterized by density ρ and Lamé coefficients λ and μ. External forces are described by the vector $(\mathbf{f}_x, \mathbf{f}_z)$. Virieux (1986) preferred to increment the τ_{xx}, τ_{zz} components of the stress tensor related to an explosive source because these components were at the same node of the staggered numerical grid (Fig. 1). We propose to follow the same strategy as Virieux (1986), and we start by detailing his implementation of an explosive source.

Let S be the infinitely small square surface surrounding the τ_{xx}, τ_{zz} location at the $(x_{i+1/2}, z_j)$ node (dashed lines in Figure 1). This surface is in equilibrium under the application of internal forces per unit length on its faces. For horizontal faces, force strength is given by: $\mathbf{f} = \mathbf{x} \cdot \tau_{zx} dL + \mathbf{z} \cdot \tau_{zz} dL$, where dL is the S square side length.

If we apply a $\Delta\tau_{zz}$ increment to τ_{zz}, the corresponding $\Delta\mathbf{f}_z$ force increments applied onto S horizontal faces are

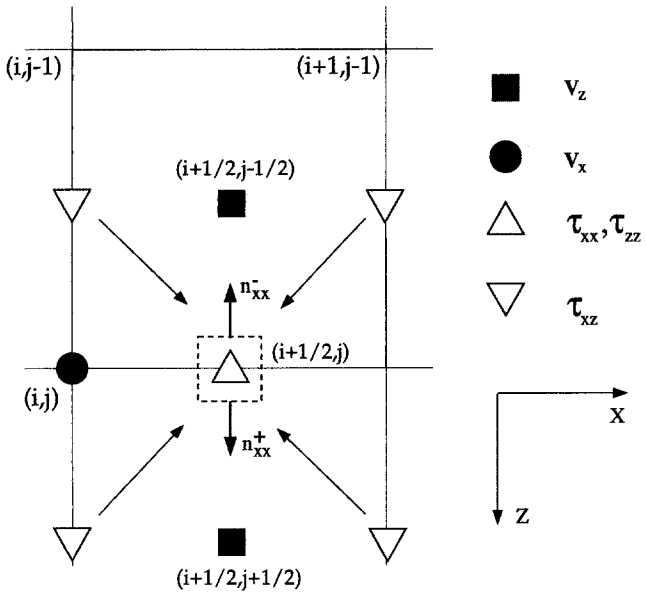

Figure 1. Discretization of the medium on a staggered grid (after Virieux, 1986). The elementary volume S is represented by dashed lines. The arrows point from the Four adjacent τ_{xz} sources added to obtain a resulting τ_{xz} source located at the $(i+1/2, j)$ node.

$$\Delta \mathbf{f}_z^+ = \mathbf{z} \cdot \Delta \mathbf{T}_z^+ dL = \mathbf{z} \cdot \mathbf{n}^+ \Delta \tau_{zz}^+ dL = \Delta \tau_{zz} dL \quad (\mathbf{z} = \text{vertical and downward unit vector}), \tag{6}$$

$$\Delta \mathbf{f}_z^- = \mathbf{z} \cdot \Delta \mathbf{T}_z^- dL = \mathbf{z} \cdot \mathbf{n}^- \Delta \tau_{zz}^- dL = -\Delta \tau_{zz} dL, \tag{7}$$

where the $^+$ ($^-$) superscript refers to the downward (upward) horizontal face of S on which $\mathbf{T}_z$ stress is evaluated. Thus, superposing a $\Delta\tau_{zz}$ increment results in applying $\Delta \mathbf{f}_z^+ - \Delta \mathbf{f}_z^- = 2\Delta\tau_{zz} dL$ vertical force discontinuity across the horizontal faces of S, that is, a $\Delta\tau_{zz} dL$ vertical dipole across $z = z_j$ surface with an a distance (or arm) between opposite forces. The same argument must be performed for $\Delta\tau_{xx}$ on an elementary length dL related to the corresponding grid step. Often, we use the same 2D finite grid step Dx for both directions, and we approximate the infinitely small surface S element by the numerical finite one. The value of the corresponding length element, dL, as well as the value of the dipole arm, a, must be estimated through comparison with exact solutions presented in the next section.

Implementing more general sources follows simply from the previous scheme but now involves stress discontinuities. Let us consider the case of a force $\mathbf{f}_z$, applied at the $(x_{i+1/2}, z_j)$ node, the τ_{zz} location. This is equivalent to applying the same force increments $\Delta \mathbf{f}_z^+ = \Delta \mathbf{f}_z^- = \Delta \mathbf{f}_z$ on the two horizontal faces of S. The stress increment, $\Delta\tau_{zz}$, is then discontinuous across the faces of S and is equal to (equations 6 and 7) the following:

$$\Delta \tau_{zz}^+ = \mathbf{f}_z / dL, \tag{8}$$

$$\Delta \tau_{zz}^- = -\Delta \mathbf{f}_z / dL. \tag{9}$$

Introducing this stress discontinuity into a second-order FD scheme is quite natural. The term τ_{zz} is used to compute the $\mathbf{v}_z$ velocity component [see equation 5 of Virieux (1986)]. The $\Delta\tau_{zz}$ stress increment is set to $-\Delta \mathbf{f}_z / dL$ when the upward τ_{zz}^- stress is employed to compute the $\mathbf{v}_z$ velocity at the $(x_{i+1/2}, z_{j-1/2})$ node, and set to $+\Delta \mathbf{f}_z / dL$ when the downward τ_{zz}^+ stress is used to compute the $\mathbf{v}_z$ velocity at the $(x_{i+1/2}, z_{j+1/2})$ node. The same strategy can be applied for the x direction, and we end up with symmetric sources with higher order of singularities than an explosive source.

Thus, in addition to the classical dipoles d_x and d_z, a dilatational source $(d_x + d_z)$, and a 45° dip-slip source $(d_x - d_z)$, we can introduce a τ_{xz} stress increment and τ_{xx}, τ_{zz}, or τ_{xz} stress discontinuities. A τ_{xz} stress increment can be identified as the sum of two c_{xz} and c_{zx} couples applied across the faces of S with opposite sign and with a moment arm of a. This represents the double-couple 90° dip-slip source. A τ_{xz} stress discontinuity, however, represents the sum of two c_{xz} and c_{zx} couples of same sign, that is, an isotropic source of S waves. All possible sources are shown in Figure 2. Because the three elementary moment tensor combinations are included, we should be able to compute any 2D dislocation of interest in seismology. However, since τ_{xx}, τ_{zz}, and τ_{xz} are not evaluated at the same position in the staggered grid, adding dipoles and double-couple sources will not result exactly in superposing the elementary moment tensor elements. Because the point $(i+1/2, j)$ plays a central role, we can, however, interpolate the four adjacent τ_{xz} values in order to obtain a symmetric solution (Fig. 1). We shall see that a careful handling of the source or receiver positions will provide an accurate symmetrical solution, and we shall give examples where this symmetry is not verified by a quantitative estimation of discrepancies induced by staggered locations.

Finally, the availability of single-force sources allows the use of reciprocal geometry in those configurations where the number of sources is much larger than the number of receivers. For a dislocation source for instance, we can compute the stress field time derivative created by a vertical (respectively horizontal) single force, instead of the vertical (respectively horizontal) velocity created by a dislocation.

Comparison with Analytical Solutions

We compare the solutions obtained by the finite difference (FD) method for dislocation sources in a homogeneous medium with exact solutions computed analytically in the frequency domain. The parameters used for computation are Vp = 6 Km/sec, Vs = 3.46 Km/sec, FD x and z grid steps = 50 m, and time step = 5 ms. The source time function is the first derivative of a Gaussian pulse, and output is given in velocity (m/sec). The geometry that we used is depicted in Figure 3. Eight receivers are distributed circularly around the source at a 500-m distance. They are located so that the receiver numbered 1, 3, 5, and 7 (respectively 2, 4, 6, and

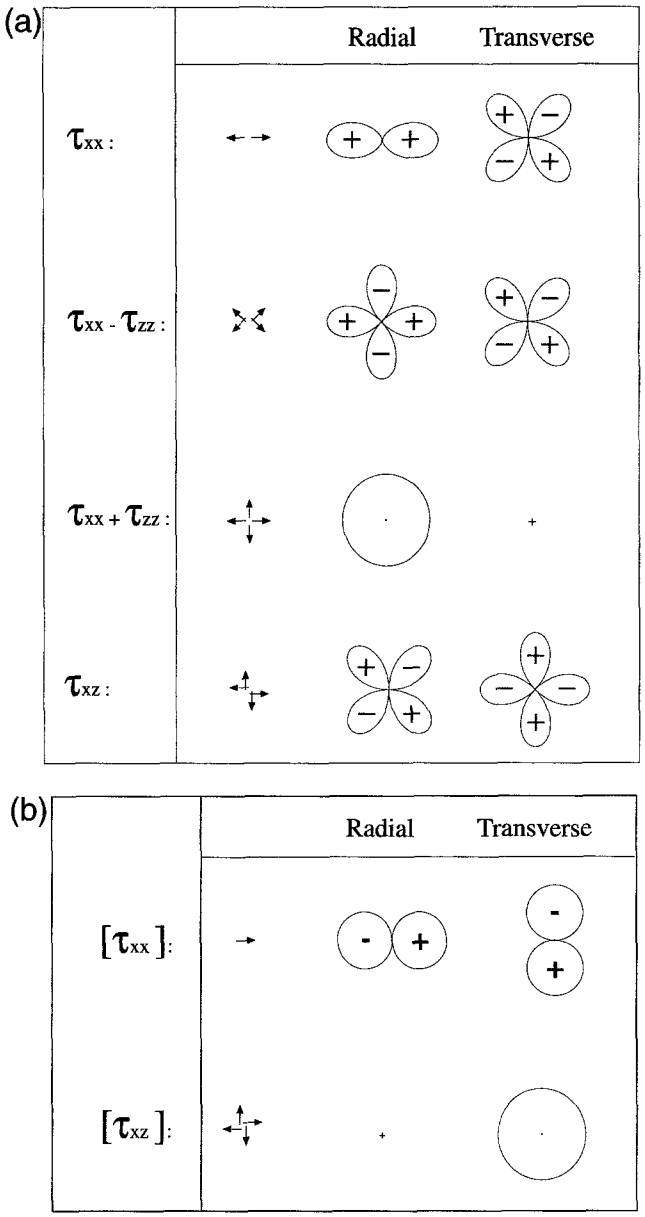

Figure 2. Diagrams showing the (a) possible stress and (b) stress-discontinuity increments with their related seismic sources and *P,S* far-field radiation patterns.

8) should exhibit identical seismograms once a sign correction is applied. The source is located at node (x_i = 200, z_i = 200), which corresponds to the location (x = 1000m, z = 1000m) in the analytical case.

In the first comparison, we have computed the velocity field radiated by a 45° dip-slip source obtained by subtracting d_x and d_z dipoles (Fig. 2). The FD exact source location is x = 1000 + $Dx/2$ = 1002.5m, z = 1000m (Fig. 1). Figure 4 shows the seismograms obtained for the vertical and horizontal components. Sites 1, 3, 5, and 7 are located in the *S*-wave nodal direction, while sites 2, 4, 6, and 8 are

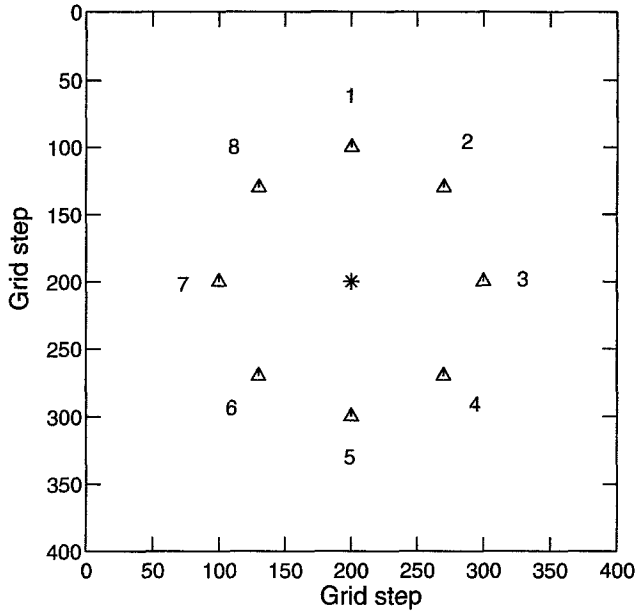

Figure 3. FD method grid size and source-receiver configuration used for computation. The source is denoted by a star, receivers by triangles.

along the *P*-wave nodal direction. Two characteristic misfits can be observed on these comparisons. The first is on arrival time discrepancy that comes essentially from the staggered grid. Velocity is not evaluated at the same location for each component, and the $d_x - d_z$ source is shifted by $Dx/2$ with respect to the analytical source location. This discrepancy can be reduced drastically, as shown in the last case, by averaging the vertical component at the horizontal component point. Second, amplitude differences are due to the numerical dispersion of the FD method and are visible mainly on the two components at sites 2, 4, 6, and 8. Notice that near-field terms are correctly evaluated in the nodal directions. An example of reciprocal computation is also shown for the vertical component at station 2. In this case, the $\tau_{xx} - \tau_{zz}$ stress time derivative, radiated by a vertical force at site 2, is computed at origin and scaled to match direct calculations. It is equivalent to the velocity computed at locations 6 and 8 due to the staggered grid.

For the second comparison, we compute the vertical and horizontal seismograms due to a dip-slip source or τ_{xz} stress increment (Fig. 5). The results are similar to the previous case. The major discrepancies arise because of time shifts due to the staggered position of the source and receivers and because of numerical dispersion. We show again an example of reciprocal calculation obtained by computing the time derivative of τ_{xz} stress at origin, radiated by a vertical source located at site 2.

The last comparison corresponds to a dislocation source computed by superposing the two previous sources with coefficients chosen to obtain a 60° dislocation (Fig. 6). In this situation, we should add the contribution of two sources with position differing by $Dx/\sqrt{2}$ (Fig. 1). We circumvent this

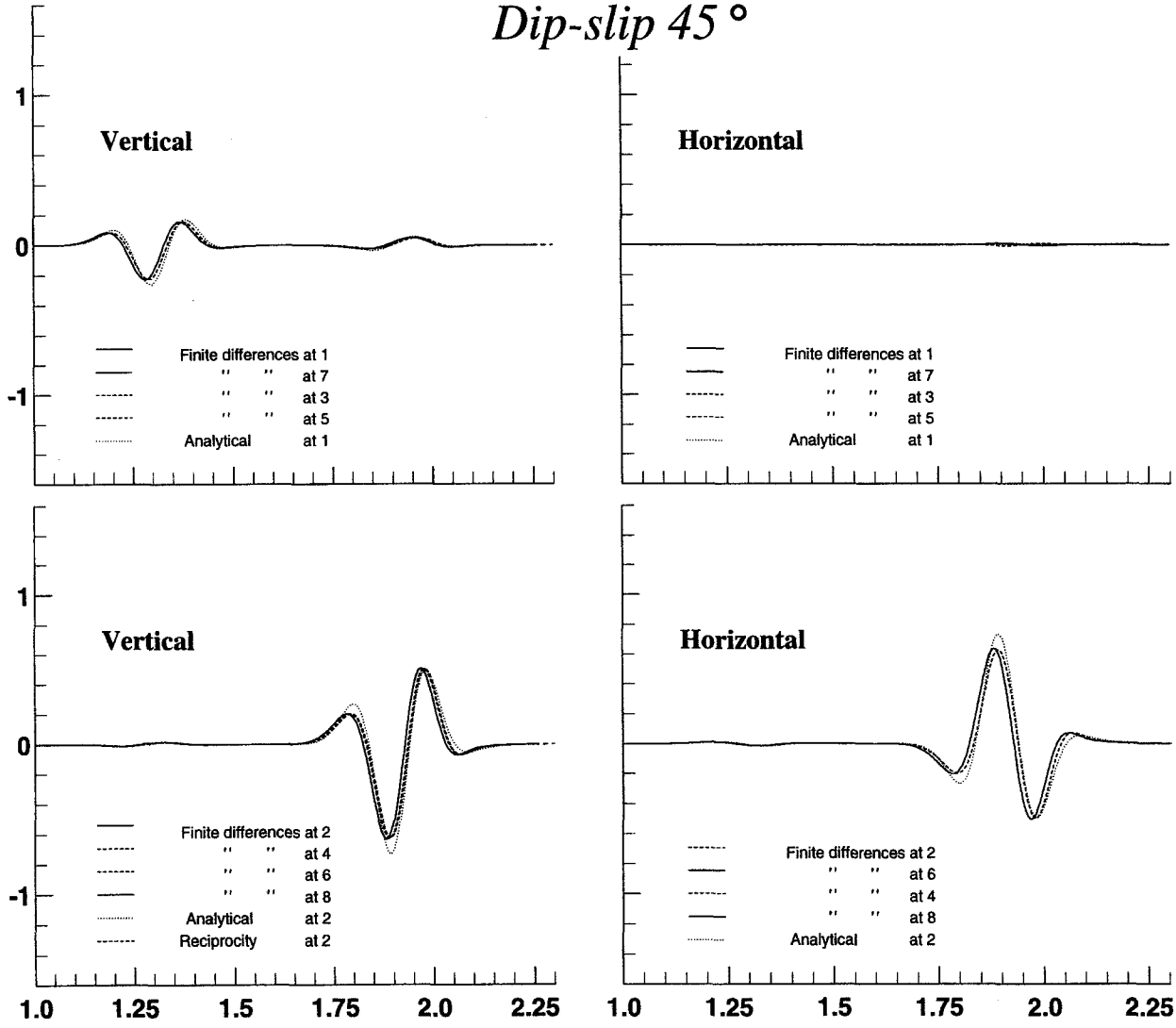

Figure 4. Results obtained for a $d_x - d_z$, 45° dip-slip source with FD and analytical methods. Time scale in seconds, amplitudes arbitrary unit. Curves having similar shape are plotted with the same pattern.

problem by averaging the four adjacent symmetrical τ_{xz} sources, as denoted by arrows on Figure 1. In the same way, we average the four symmetrical vertical components to evaluate them at the (x_i, z_j) location. Seismograms are computed for the vertical and horizontal components at sites 1 and 2, and the analytical source is shifted by an amount $Dx/2$ to account for the FD exact source location. The results shown on Figure 6 present an excellent agreement where the only misfits are due to FD numerical dispersion.

The output of the analytical computations have been obtained as the velocity produced by normalized dipoles or couples of 1 Nm. The source in FD, however, is introduced as a stress or stress discontinuity. Thus, scaling FD amplitudes to analytical amplitude involves the following conversion: from stress to force, multiplying by the dL length; from force to dipole/moment, multiplying by the a moment arm. We found that the results scale through a Dx^2 proportionality coefficient. The lengths of both couple and dipole arms and surface elements in the (Ox, Oz) plane are thus equal to the grid step Dx.

Discussion and Conclusions

We have studied the numerical implementation of seismic sources in the staggered numerical grid for an FD scheme of second order.

We have shown that the numerical solution agrees with the analytical solution when the elementary surface on which we apply the stress is taken as the grid step Dx and when the elementary dipole/couple arm when needed is also equal to the grid step Dx. Of course, this estimation depends on the order of the FD scheme, or in other words, it depends on the interpolation used to estimate any field between nodes.

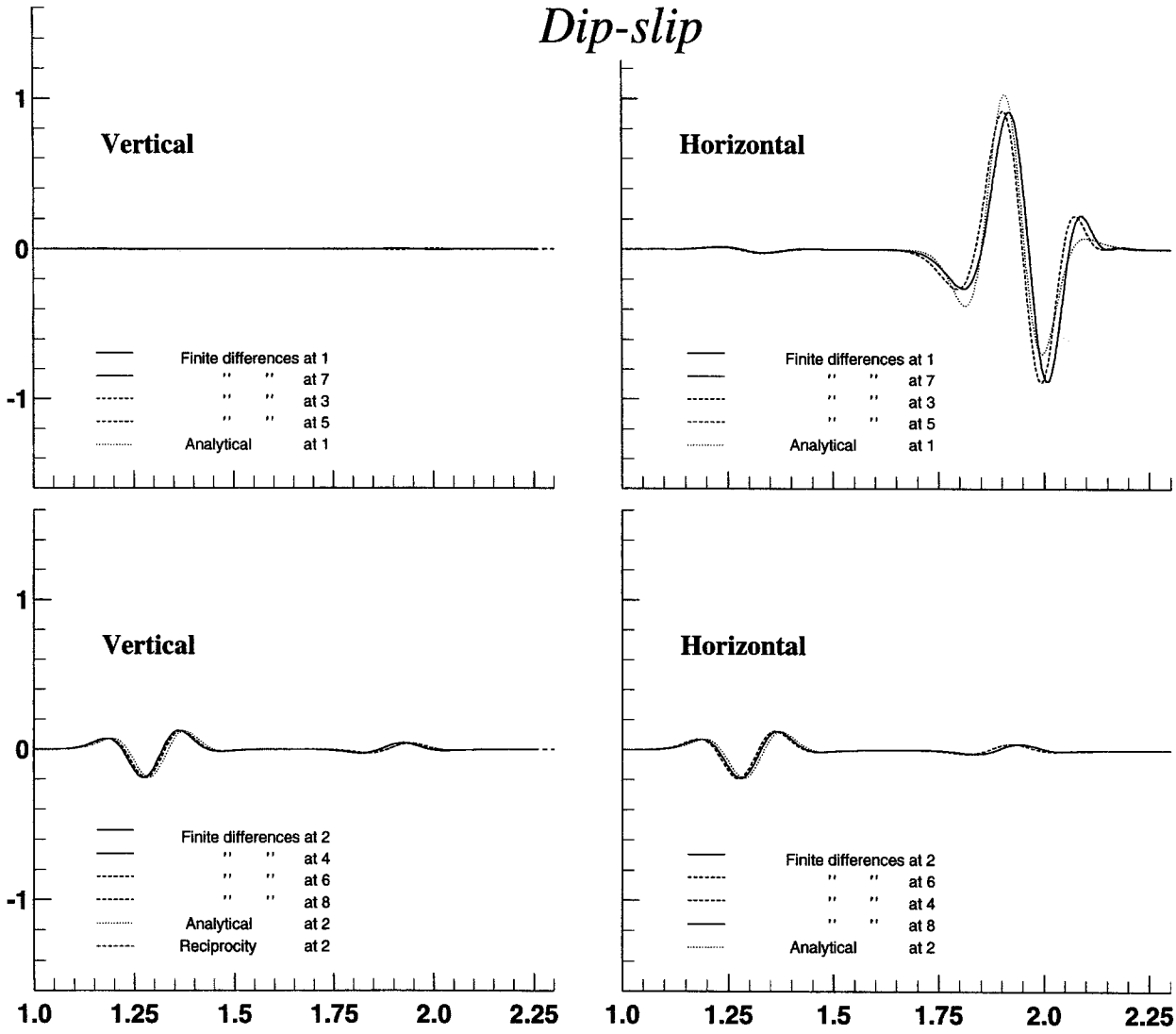

Figure 5. Same as Figure 4 for a τ_{xz} dip-slip source.

This result is a new result coming from a careful comparison between numerical and analytical seismograms.

Moreover, selecting the τ_{xx} and τ_{zz} node as the source node reduces significantly the grid asymmetry. A linear weighting between the four adjacent nodes where the stress component τ_{xz} is preserves the symmetry of the point source excitation.

Application to real data set requires a conversion from the 2D geometry toward a 3D geometry. While this transformation can be performed quite accurately for horizontally layered media, as proposed by Amundsen and Reitan (1994), investigation for more complex structures has to be designed and will be the purpose for a future work.

Acknowledgments

We thank Jeff Barker and John Vidale for critically reviewing the manuscript.

References

Alford, R., K. Kelly, and D. Boore (1974). Accuracy of finite-difference modeling of the acoustic wave equation, *Geophysics* **39**, 834–842.

Alterman, Z., and F. Karal (1968). Propagation of elastic waves in layered media by finite difference methods, *Bull. Seism. Soc. Am.* **58**, 367–398.

Amundsen, L. and A. Reitan (1994). Transformation from 2-d to 3-d wave propagation for horizontally layered media, *Geophysics* **59**, 1920–1926.

Bayliss, A., K. Jordan, J. LeMesurier, and E. Turkel (1986). A fourth-order accurate finite-difference scheme for the computation of elastic waves, *Bull. Seism. Soc. Am.* **76**, 1115–1132.

Crase, E. (1990). High order (space and time) finite-difference modeling of the elastic wave equation, Presented at the 60th annual meeting of the SEG expanded abstracts, San Francisco, September 23–27, pp. 987–991.

Dablain, M. (1986). The application of high-order differencing to the scalar wave equation, *Geophysics* **51**, 54–66.

Holberg, O. (1987). Computational aspects of the choice of operator and sampling interval for numerical differentiation in large-scale simulation of wave phenomena, *Geophys. Prospect.* **35**, 629–655.

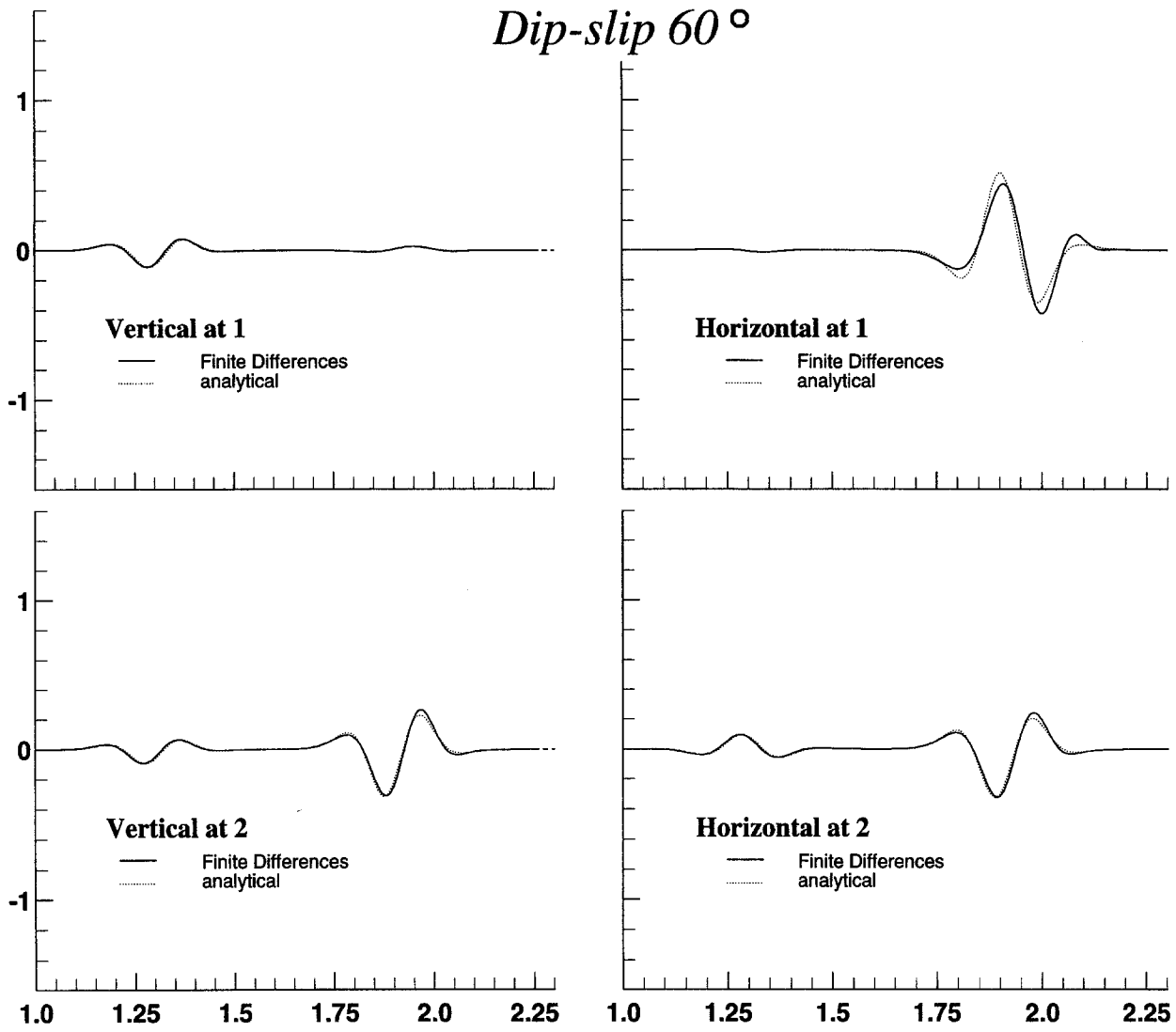

Figure 6. Results obtained for a 60° dip-slip source where four adjacent τ_{xz} sources and four adjacent vertical components are averaged to solve for source and component staggered locations at sites 1 and 2.

Kelly, K., R. Ward, S. Treitel, and R. Alford (1976). Synthetic seismograms, a finite difference approach, *Geophysics* **41**, 2–27.

Kosloff, D. and E. Baysal (1982). Forward modeling by a fourier method, *Geophysics* **47**, 1402–1412.

Kosloff, D., A. Filho, E. Tessmer, and A. Behle (1989). Numerical solution of the acoustic and elastic wave equations by a new rapid expansion method, *Geophys. Prospect.* **37**, 383–394.

Kosloff, D., M. Reshef, and D. Loewenthal (1984). Elastic wave calculations by the fourier method, *Bull. Seism. Soc. Am.* **74**, 875–891.

Levander, A. (1988). Fourth-order finite-difference p-sv seismograms, *Geophysics* **53**, 1425–1436.

Vidale, J. and D. Helmberger (1987). Path effects in strong motion seismology, in *Seismic Strong Motion Synthetics*, B. Bolt (Editor), Academic Press, New York, 267–308.

Virieux, J. (1984). Sh-wave propagation in heterogeneous media: velocity-stress finite-difference method, *Geophysics* **49**, 1933–1942.

Virieux, J. (1986). P-sv wave propagation in heterogeneous media: velocity-stress finite-difference method, *Geophysics* **51**, 889–901.

Universite Joseph Fourier
Lab de Geophysique Interne et Tectonophysique
BP 53X
38041 Grenoble Cedex, France
(O.C.)

Institut de Ge'odynamique
UNSA
Valbonne, France
(J.V.)

Departmente Geofisica e Vulcanologia
Napoli, Italy
(A.Z.)

Manuscript received 21 November 1994.